Molecular Neurobiology (2019) 56:4639–4652
https://doi.org/10.1007/s12035-018-1404-2

Removal of p75 Neurotrophin Receptor Expression from Cholinergic Basal Forebrain Neurons Reduces Amyloid-β Plaque Deposition and Cognitive Impairment in Aged APP/PS1 Mice

Lei Qian[1,2] · Michael R. Milne[1,2] · Stephanie Shepheard[3] · Mary-Louise Rogers[3] · Rodrigo Medeiros[1] · Elizabeth J. Coulson[1,2]

Received: 22 May 2018 / Accepted: 22 October 2018 / Published online: 29 October 2018

Abstract

The degeneration of cholinergic basal forebrain (cBF) neurons in Alzheimer's disease (AD) leads to the cognitive impairment associated with this condition. cBF neurons express the p75 neurotrophin receptor ($p75^{NTR}$), which mediates cell death, and the extracellular domain of $p75^{NTR}$ can bind to amyloid beta (Aβ) and promote its degradation. Here, we investigated the contribution of cBF neuronal $p75^{NTR}$ to the progression of AD by removing $p75^{NTR}$ from cholinergic neurons in the APP/PS1 familial AD mouse strain. Conditional loss of $p75^{NTR}$ slowed cognitive decline and reduced both Aβ accumulation into plaques and gliosis. Expression of the amyloid protein precursor and its cleavage enzymes ADAM10 and BACE1 were unchanged. There was also no upregulation of $p75^{NTR}$ in non-cholinergic cell types. This indicates that a direct interaction between cBF-expressed $p75^{NTR}$ and Aβ does not contribute significantly to the regulation of Aβ load. Rather, loss of $p75^{NTR}$ from cBF neurons, which results in increased cholinergic innervation of the cortex, appears to regulate alternative, more dominant, Aβ clearance mechanisms.

Keywords Cholinergic basal forebrain · p75 neurotrophin receptor · Alzheimer's disease · Cognitive impairment · Amyloid plaque · p75 extracellular domain · Conditional knockout

Introduction

The core features of Alzheimer's disease (AD) include the accumulation of amyloid-beta (Aβ) in the brain (particularly in the cortex), cognitive impairment, and neurodegeneration [1], with the selective death of cholinergic basal forebrain (cBF) neurons emerging as a potential mediator of both cognitive impairment and Aβ production and/or accumulation. In humans, cBF neuronal degeneration causes basal forebrain atrophy that can be measured as a decrease in MRI volume of the nuclei. This loss is an early hallmark of AD [2–5], and it precedes and is correlated with Aβ load as well as cognitive impairment [4, 6–11]. In animal models of familial AD that overproduce Aβ, lesioning of cBF neurons in pre-symptomatic or middle-aged mice causes exacerbation of Aβ pathology and cognitive decline, and can result in hippocampal degeneration [12–17]. In an apparent vicious cycle, Aβ is also neurotoxic to cBF neurons [18–22].

cBF neurons are characterized by the expression of the p75 neurotrophin receptor ($p75^{NTR}$), which is well known for its role in mediating cell death [23–25]. In the context of AD, $p75^{NTR}$ can directly interact with Aβ, resulting in internalization of the peptide within cBF neurons [20, 21, 26–28]. Aβ binding to $p75^{NTR}$ can also activate cell death pathways, mediating Aβ-induced cBF degeneration [18, 29–34]. Blocking or modulating $p75^{NTR}$ signaling with small molecules that interact with the $p75^{NTR}$ extracellular domain ($p75^{ECD}$) or complete $p75^{NTR}$ gene deletion reduces cBF degeneration in Aβ-overexpressing transgenic mice [18–20]. Modulation of $p75^{NTR}$ signaling also has positive effects on spatial navigation performance in both wild-type and transgenic mice that overproduce Aβ (see Table 1 [19, 36–41]). These and other studies highlight $p75^{NTR}$ as a candidate therapeutic target for

✉ Elizabeth J. Coulson
e.coulson@uq.edu.au

[1] Queensland Brain Institute, Clem Jones Centre for Ageing Dementia Research, The University of Queensland, Brisbane, QLD 4072, Australia

[2] School of Biomedical Sciences, The University of Queensland, Brisbane, QLD 4072, Australia

[3] Centre for Neuroscience, College of Medicine and Public Health, Flinders University, Adelaide, SA 5001, Australia

Table 1 Summary of disease features of AD mice with reduced $p75^{NTR}$ gene expression or function

Reference	Mouse strain	Cognitive performance	Aβ plaques	Aβ ELISA
Knowles et al. 2009 [20]	c57BL6 Thy1-hAPP$^{Lond/Swe}$ $p75^{exonIII-/-}$	–	No change in hippocampal or cortical plaque load	No change in Aβ in hippocampus and cortex
Wang et al. 2011 [35]	sv129 APP/PS1 $p75^{exonIII-/-}$	No change	Increased number of Aβ plaques at 9 months	Increased total Aβ from 6 months of age. Decreased soluble Aβ (TBS extracted fraction) at 9 months
Knowles et al. 2013 [19]	c57BL6 Thy1-hAPP$^{Lond/Swe}$ LM11A-31 treatment	Improved performance in novel object recognition and Y-maze alternation at 7–8 months	–	No change in Aβ
Nguyen et al. 2014 [36]	c57BL6 Thy1-hAPP$^{Lond/Swe}$ LM11A-31 treatment	Improved learning in Morris water maze and contextual fear conditioning at 6–7 months.	No change in Aβ deposition	–
Murphy et al. 2015 [37]	sv129 Tg2576 $p75^{exonIII-/+}$	Improved performance in cued fear conditioning and Barnes maze	–	Increased levels of insoluble Aβ. No significant change in soluble Aβ
Jian et al. 2016 [38]	c57BL6 Tg2576 $p75^{exonIII-/+}$	Improved performance in Morris water maze	Reduced Aβ plaque deposition	Decreased Aβ42
This paper	c57BL6 APP/PS1 ChAT-cre $p75^{in/in}$	Improved performance in active place avoidance task at 13 months	Reduced Aβ plaque deposition at 13 months	No change in total Aβ42

the treatment of the cholinergic degeneration associated with dementia [42–44].

In the above studies, the cognitive improvements linked to inhibition of $p75^{NTR}$ function were usually not accompanied by effects on Aβ plaque size or density (Table 1; [19, 36, 37]). However, one study has reported that knockout of $p75^{NTR}$ in APP/PS1 (amyloid precursor protein/presenilin 1) mice results in significantly increased levels of cortical Aβ and exacerbated cognitive decline [35]. The authors proposed that $p75^{ECD}$, a marker of neurodegeneration [45, 46], can help to clear Aβ from the brain by binding it and preventing its aggregation [35, 47]. This idea is supported by the results of subsequent studies [48, 49], which have reported that the treatment of aged APP/PS1 mice with a $p75^{NTR}$ extracellular domain fragment improves cognitive impairment coincident with reduced Aβ load. Using drugs to prevent Aβ-induced cBF neuronal degeneration by blocking $p75^{NTR}$, death signaling could therefore have counterproductive effects through the exacerbation of cortical Aβ levels.

To better understand the role of cBF neuronal $p75^{NTR}$ on Aβ levels, we crossed mice from our conditional, cholinergic-specific $p75^{NTR}$ knockout mice (ChAT-cre: $p75^{fl/fl}$ [39]) with familial AD APP/PS1 transgenic mice, and assessed the Aβ load and cognitive performance of their offspring.

Materials and Methods

Mice

All procedures were approved by the University of Queensland Animal Ethics Committee and conducted in accordance with the Australian Code of Practice for the Care and Use of Animals for Scientific Purposes. The animal facility was kept on a 12 h–12 h light-dark cycle. Animals were housed up to five per cage and were provided ad libitum access to water and food. Where mice required separation for welfare reasons, they were separated by a visual- and olfactory-permeable barrier. Animals and samples were randomized when possible. Male littermate mice were used at the ages indicated.

The double transgenic APP/PS1 (B6.Cg-Tg(APPswe,PSEN1dE9)85Dbo, JAX - 34,832) mice carry two transgenes. One of these transgenes encodes a chimeric human APP with the Swedish mutations K595N/M596L (APPswe), and the other encodes human PS1 with the DeltaE9 mutation (PSEN1dE9). The mice were backcrossed to C57BL6 animals for more than ten generations. The $p75^{NTR}$ conditional "flexed" knockout ($p75^{fl/fl}$) mouse was generated based on C57BL6 embryonic stem cells as previously described [39]. The $p75^{NTR}$ gene was knocked out in all cholinergic neurons, including motor neurons and those in the basal forebrain, by inversion of exon 1 ($p75^{in/in}$) by intercrossing with the C57BL6 mouse strain in which cre recombinase expression is driven by the choline acetyltransferase (ChAT) promoter (B6.129S6-$Chat^{tm2(cre)Lowl}$/J, JAX - 6410). No overt motor phenotype was observed in these mice. Other cholinergic populations such as the striatum and mesopontine nuclei do not normally express $p75^{NTR}$ and we therefore expect that their function would be unaffected.

cBF Neuron Lesioning

Mice were anesthetized by intraperitoneal (i.p.) injection of ketamine (100 mg/kg) and xylazine (10 mg/kg). To lesion cBF neurons, a single infusion of murine p75-saporin (0.4 mg/ml; Advanced Targeting Systems) or control rabbit IgG-saporin (0.4 mg/ml) was stereotaxically injected into the basal forebrain. The needle was lowered into the medial septum (A-P 0.9 mm; M-L 0 mm; D-V 4.2 mm from Bregma) and the toxin was infused at a rate of 0.4 μl/min (1.5 μl total volume).

Y-maze

The Y-maze task was used to test working spatial memory. The Y-maze was composed of three equally spaced arms (120° apart, 35 cm long and 10 cm wide) made of perspex. The maze was positioned 1 m above the ground. During training, the mice were placed in one of the arms (the start arm) with access to only one other arm for a period of 15 min. The training arm alternated between mice. One day after the training, mice were allowed to explore in the Y-maze for 10 min with access to all three arms. Animals were tracked using EthoVision XT software and the total time and the percent time spent in each arm were analyzed for both the first 3 min and throughout the full all 10-min period.

Active Place Avoidance

The active place avoidance task was used to test allothetic spatial learning and memory [50, 51], as it is considered to be less stressful for older mice than the Morris water maze. The apparatus (Bio-Signal Group) was located in a room with visual cues on the walls and consisted of an arena (80 cm diameter, 20 cm high) with a transparent circular boundary placed on a square grid of parallel metal rods (4 mm diameter, 5 mm apart) on a stainless steel Table 1 meter above the floor. Light levels were maintained at 35 Lux throughout the experiment. An overhead camera (Flea2, Pointgrey) was used to track the position of the animal in the apparatus. Behavior was analyzed using Track Analysis software (Bio-Signal Group). The arena rotated clockwise at a speed of 1 rpm and an electric shock could be delivered through the grid floor. On day one, all mice underwent a habituation session during

which they were allowed to explore the arena freely for 5 min without receiving any shocks. They then underwent daily 10 min training sessions for 5 days, in which they were placed in the arena and trained to avoid a 60° shock zone, the positioning of which was kept constant in relation to the room coordinates. Entrance into the shock zone led to the delivery of a brief foot shock (500 ms, 0.5 mA). If, after the initial shock, the animal remained in the shock zone, further shocks were delivered at 1.5 s intervals until it moved out of the zone. To determine their memory of the shock zone, 24 h after the final training session, the mice were allowed to explore the arena for 10 min without shocks being applied.

Recorded tracks were analyzed offline using Track Analysis software. In order to assess the extent of learning, the following parameters were measured: number of foot shocks, maximal avoidance time of the shock zone, and latency to first entry into the shock zone. Animals were excluded from the analysis if they failed to respond to the foot shock during training sessions by attempting to avoid the shock area.

Immunohistochemical and Histochemical Studies

Following phenotypic analyses, the experimental animals were deeply anesthetized with sodium pentobarbitone, 200 mg/kg i.p.) and transcardially perfused with 30 ml of 0.1 M phosphate buffered saline (PBS, pH 7.4) containing 1% sodium nitrite, followed by 30 ml of 4% paraformaldehyde (PFA) in PBS. Brains were post-fixed with 4% PFA overnight and, after repeated washing in PBS, preserved in 30% sucrose solution for 24 h. Coronal or sagittal sections (40 μm) were cut in three serially adjacent sets through the basal forebrain and hippocampus using a sliding microtome (SM2000r, Leica). Sections were stored in 0.1% sodium azide in 0.1 M PBS.

For immunofluorescence labeling, free-floating sections were probed using a range of antibodies followed by the appropriate secondary antibody (1:1000, Life Technologies). Sections from $p75^{KO}$ mice were stained using anti-extracellular $p75^{NTR}$ (1:400, AF1157, R&D Systems), rabbit anti-DsRed (1:200; Clontech), and goat anti-ChAT (1:1000; ab144P, Millipore). Amyloid plaques were visualized using mouse anti-Aβ (6E10, 1:500, Sig-39320, Convance), or incubated with 0.1% thioflavin S in water (T1892, Sigma-Aldrich). Astrocytes were labeled using anti-GFAP (1:500, Z0334, Dako), and microglia were visualized using anti-CD68 (MCA1957, AbD Serotec). Sections were mounted onto slides and coverslipped using fluorescence mounting medium (Dako). For quantification of cholinergic axons, goat anti-ChAT (1:400, ab144P, Merck Millipore) biotinylated donkey secondary antibodies (1:1000, Jackson Immunoresearch Laboratories) and ABC reagent (Vector Laboratories) were applied sequentially with washing steps in-between. Immunocytochemical labeling was visualized using nickel-intensified DAB (3,3′-diaminobenzidine) staining. Brain slices were mounted on slides and coverslipped with DePex (Sigma-Aldrich).

Image Analysis and Histological Quantification

Images of histological sections were obtained using either an upright fluorescence slide scanner (Zeiss Axio Imager Z2) with a × 20 objective and AxioVision software, or a Yokogawa spinning disk confocal microscope with a × 20 objective and sequential acquisition settings at 1024 × 1024 pixel resolution controlled by Slidebook 6.0 software.

For all histological quantification experiments, a minimum of three mice were used for each genotype at each age. All basal forebrain cell counts were performed from 1.3 to 0.1 mm anterior to bregma, with every third section being analyzed. The percentage area occupied by Aβ plaques, astrocytes, and microglia in the entire neocortical region per section was determined with an Imaris 7 software (Bitplane) and the values for five sections per mouse were averaged for each mouse and then each genotype. Quantification of cBF axonal density has been previously described in detail [39]. Essentially, images were converted to black and white and the area covered by immunopositive axons was calculated for a defined region of interest.

Biochemical Assays

For biochemical analyses, mice were perfused with PBS before sacrifice by cervical dislocation. The brains were removed and the cortex and hippocampus were dissected, weighed, and snapfrozen with liquid nitrogen. Protein was extracted by adding 20 *v/w* lysis buffer (0.05 M sodium acetate, 1 M sodium chloride, 1% bovine serum albumin, 1% Triton-X100, Roche complete inhibitor cocktail tablet) to the tissue before homogenization using a Bullet Blender Storm 24 (Next Advance). The level of Aβ42 in the tissue was assessed by ELISA as per the manufacturer's instructions (Biosensis). The resulting measurements were normalized for tissue weight. Proteins within the tissue lysates (150 μg) were also electrophoresed, and the resultant western blots probed for APP (1:5000, 1565-1, Epitomics), BACE1 (1:1000, 195111, Merck Millipore), ADAM10 (1:1000, ab124695, Abcam), and ChAT (1:2000, ab144P, Merck Millipore) with appropriate secondary antibodies. Immunoreactive bands were visualized and quantified using Image Studio™ Lite v5.2.5 (LI-COR Biosciences) normalized to GAPDH (1:4000, 2118, Cell Signaling Technology).

To measure the peripheral levels of the extracellular domain fragment of $p75^{NTR}$ ($p75^{ECD}$), a sandwich ELISA that captures $p75^{ECD}$ from mouse urine was used, as previously described [52, 53]. Briefly, ELISA plates (96-well plates, Costar Corning) were coated for 18 h at 4 °C with 4 μg/ml

mouse anti-p75^{ECD} (MLR1) in 25 mM sodium carbonate, 25 mM sodium hydrogen carbonate, and 0.01% thimerosal, pH 9.6. Wells were blocked with sample buffer comprising PBS, 2% bovine serum albumin (Sigma) and 0.01% thimerosal, pH 7.4, for 1 h at 37 °C. Recombinant mouse p75^{ECD} (control antigen, aa:20-243, R&D Systems) and urine samples were diluted in sample buffer and incubated for 20 h at room temperature. Wells were then incubated with goat anti-p75^{ECD} (R&D Systems) for 1 h followed by a bovine anti-goat IgG-HRP antibody (Jackson ImmunoResearch) for 1 h at room temperature. Visualization was achieved via a peroxidase reaction developed using the color reagent 3,3′,5,5′-tetramethylbenzidine (Bio-Rad) and stopped with 2 M sulfuric acid. Between steps, plates were washed four times with wash buffer (PBS, 0.05% Tween 20, 0.01% thimerosal, pH 7.4). Plates were read at 450 nm with a PerkinElmer Victor-× 4 Plate Reader. Mouse creatinine was used as a standard for urinary protein measurements and was assessed using a creatinine detection kit (Enzo Life Sciences) as previously described [53].

Statistics

Statistical analysis was performed using GraphPad Prism 7 software, accounting for appropriate distribution and variance to ensure that correct statistical parameters were applied. The statistical analysis are described in the figure legends or text for the respective experiments. Values are expressed as the mean ± SEM, with significance set at $p < 0.05$. No statistical methods were used to predetermine sample sizes. Sample size was determined on the basis of our previous knowledge of likely effect size, but varied between experiments due to littermate genotypes, gender, and the survival of the animals to 14 months of age.

Results

ChAT-cre$^{+/-}$: p75$^{in/in}$ mice (p75^{KO}) were crossed with APP/PS1$^{+/-}$ (APP/PS1) mice to generate ChAT-cre$^{+/-}$: p75$^{in/in}$: APP/PS1$^{+/-}$ (p75^{KO}APP/PS1) mice and cre-negative, control homozygous p75$^{fl/fl}$ (p75$^{fl/fl}$) littermates (Table 2). Immunohistochemistry for p75^{NTR} or mCherry, the expression of which occurs in place of p75^{NTR} when the cre enzyme inverts ("$^{in/in}$") the *floxed* allele of p75^{NTR} ([39], Fig. 1a), was undertaken on basal forebrain sections to confirm that the p75^{KO} APP/PS1 mice were deficient for p75^{NTR}. The vast majority (~ 87%) of ChAT-positive cells in the basal forebrain of adult p75^{KO}APP/PS1 animals were also positive for mCherry, and did not express p75^{NTR} (Fig. 1b, c; ChAT: 132.8 ± 14.4 cells/section vs mCherry: 116.5 ± 13.5 cells/section), which is consistent with our previous report of the p75^{KO} mouse model [39]. In ChAT-cre: p75$^{in/in}$ mice, the p75^{NTR} gene is interrupted from postnatal day 4, prior to the period of naturally occurring basal forebrain cell death, resulting in a 25% increase in cell number and increased cholinergic axonal innervation in layer 5 of the cortex compared with control p75$^{fl/fl}$ mice [39]. A similar trend was observed in our experimental cohort (Fig. 1d, e). In addition, APP/PS1 mice displayed significantly reduced ChAT immunostaining of cBF axons in the cortex compared to p75^{KO} mice, with p75^{KO}APP/PS1 mice having innervation equivalent to that of p75$^{fl/fl}$ controls.

To determine whether cBF p75^{NTR} deficiency affected cognitive ability, a cohort of 13-month-old mice was first tested for memory performance in the Y-maze. No significant differences between genotypes was found in time spent in the novel arm (two-way ANOVA followed by Sidak's multiple comparison test, interaction: $F(1,16) = 0.0929$, $p = 0.7644$; genotype: $F(1,16) = 2.705$, $p = 0.1195$). Next, the mice were tested in the hippocampal memory-dependent active place avoidance paradigm [54]. In this task, the mice were trained to avoid a shock zone over 5 days in a rotating arena (Fig. 2a). On the 6th day, they were returned to the arena but no shocks were applied on entrance to the shock zone; however, the number of shocks they would have received ("shocks") was recorded. Animals of all four genotypes traveled an equivalent distance within the arena during this task (Fig. 2b; two-way ANOVA followed by Tukey's multiple comparison test, interaction: $F(12,96) = 0.7195$, $p = 0.7292$; genotype: $F(3,24) = 1.591$, $p = 0.2176$). During the training period, the number of shocks received by control (p75$^{fl/fl}$) and p75^{KO} mice reduced with time (two-way ANOVA followed by Tukey's multiple comparison test, interaction: $F(12,96) = 0.6586$, $p = 0.7865$; genotype: $F(3,24) = 9.4760$, $p = 0.0003$), coincident with an increase in the maximal time between shocks (Fig. 2c, d; two-way ANOVA followed by Tukey's multiple comparison test, interaction: $F(12,96) = 0.5835$, $p = 0.8507$; genotype: $F(3,24) =$

Table 2 Genotypes of the parents and experimental progeny used in this study and the abbreviated nomenclature

APP/PS1$^{+/-}$; p75$^{fl/fl}$ X ChAT-cre$^{\pm}$; p75$^{fl/fl}$	*ChAT-cre^{+}; p75fl*	*ChAT-cre^{-}; p75fl*
APP/PS1^{+}; p75fl	APP/PS1^{+}; ChAT-cre^{+}; p75$^{in/in}$ **p75^{KO}APP/PS1**	APP/PS1^{+}; ChAT-cre^{-}; p75$^{fl/fl}$ **APP/PS1**
APP/PS1^{-}; p75fl	APP/PS1^{-}; ChAT-cre^{+}; p75$^{in/in}$ **p75^{KO}**	APP/PS1^{-}; ChAT-cre^{-}; p75$^{fl/fl}$ **p75$^{fl/fl}$**

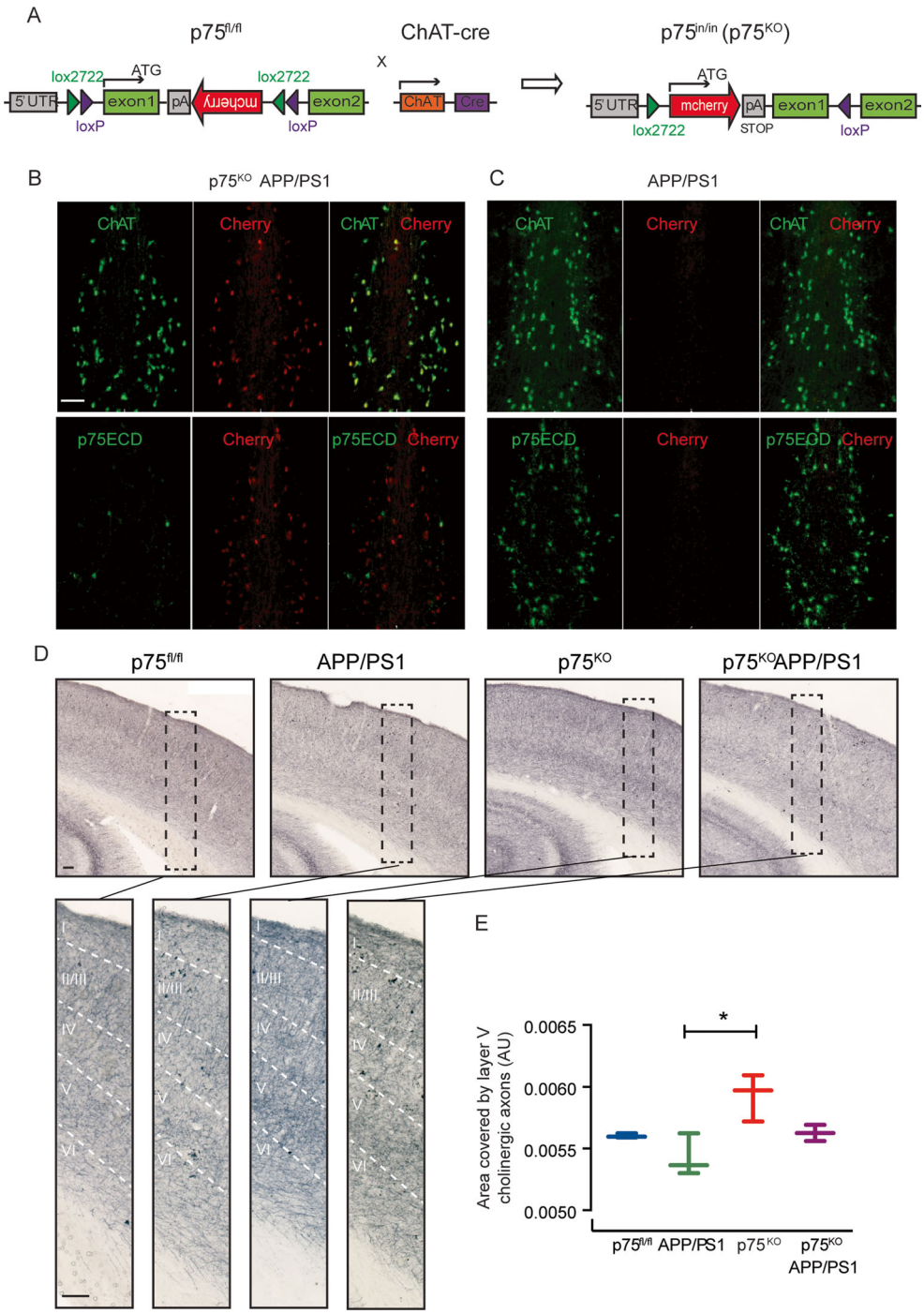

Fig. 1 **a** Diagram of the p75^{NTR} *flexed* allele before and after recombination due to ChAT-cre expression. On recombination, p75^{NTR} exon 1 is inverted and mCherry is expressed instead. Immunofluorescence images of basal forebrain sections from **b** p75^{KO}APP/PS1 and **c** APP/PS1 mice. Sections are costained for mCherry (red) and either ChAT or the p75^{NTR} extracellular domain (p75ECD; green), confirming that significant recombination of both p75^{NTR} alleles has occurred in the p75^{KO}APP/PS1 mice. **d** High and low power images of cortical sections of p75^{KO}APP/PS1 and control mice stained for ChAT. Scale bars 100 μm. **e** Quantification in arbitrary units (AU) of the area that is immunopositive for ChAT in layer V of the somatosensory cortex of 13-month-old mice. (*$p < 0.05$; one-way ANOVA, Tukey's multiple comparisons test. $N = 3$ animals per group)

4.711, $p = 0.0101$), indicative of learning. In contrast, APP/PS1 mice did not exhibit learning (Fig. 2c, d) and, on the test day, their time to first entrance to the previous shock zone was shorter and they entered this zone more often and/or spent a longer period of time there than the age-matched control mice, and thereby received significantly more "shocks" (Fig. 2e, f; one-way ANOVA followed by Tukey's multiple comparison test, time to first shock: $F(3,24) = 4.482$, $p = 0.0123$; number of "shocks": $F(3,24) = 5.081$, $p = 0.0073$). However, the p75^{KO}APP/PS1 mice displayed an intermediate phenotype in both the learning and memory phases of the paradigm (Fig. 2c–f), receiving significantly fewer "shocks" than APP/PS1 mice on the test day (Fig. 2f; p75^{KO}APP/PS1 vs APP/PS1: $p = 0.0430$). This suggests that the loss of cholinergic neuronal p75^{NTR} in aged APP/PS1 mice benefits cognitive processes.

We next investigated whether the deletion of p75^{NTR} in APP/PS1 mice affected the accumulation of Aβ over time. Aβ plaque burden in histological sections was visualized using thioflavin S staining and immunolabeling with the

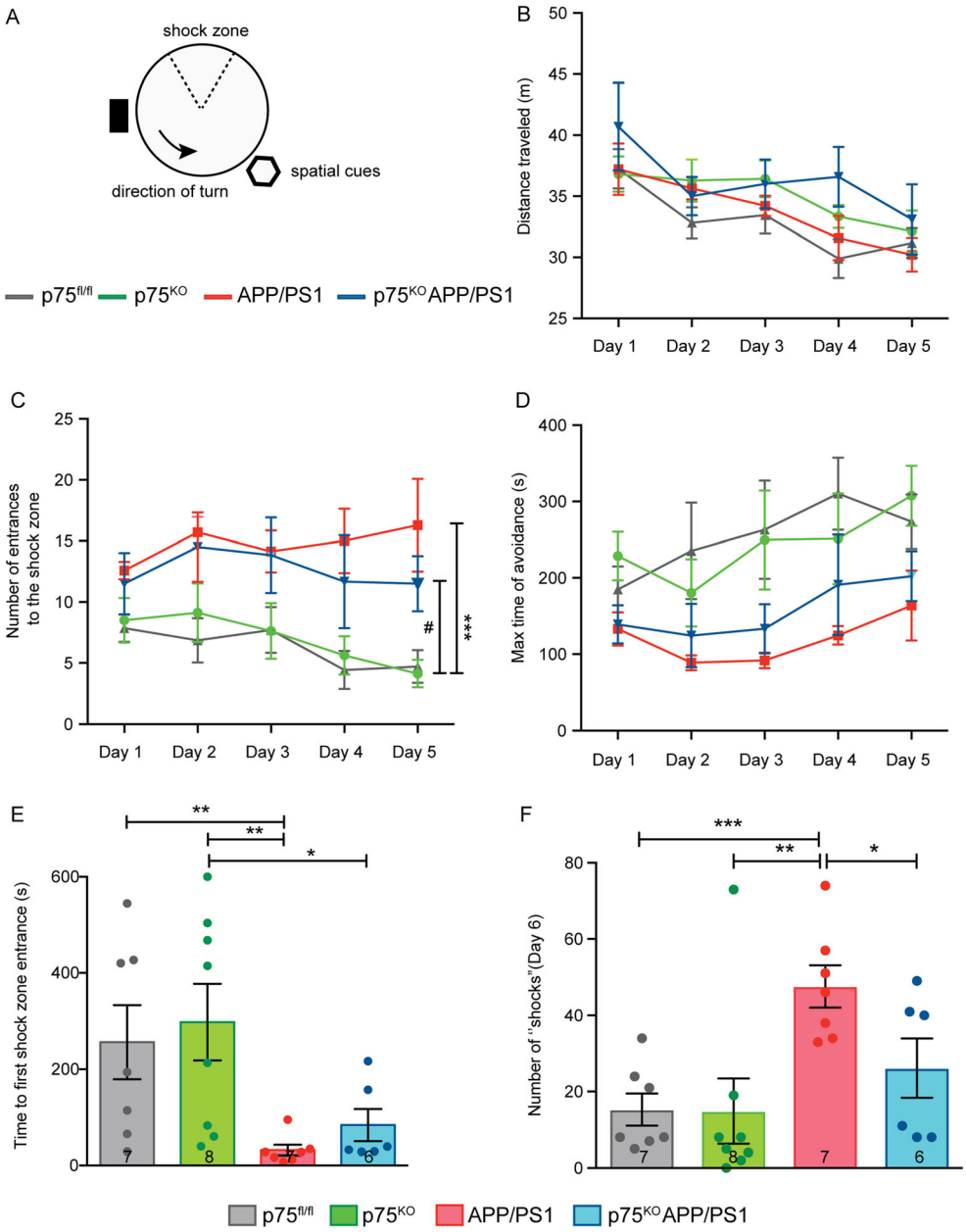

Fig. 2 **a** Diagram of the top view of the active place avoidance navigation task. **b** Quantification of the distance traveled, **c** number of entrances to the shock zone, and **d** maximum time of avoidance of the shock zone of 13-month-old mice during their 5 days of training. #p75^{KO}APP/PS1 vs p75^{KO} is not significantly different whereas p75^{KO}APP/PS1 vs p75$^{fl/fl}$ $p = 0.047$; ***$p < 0.001$; two-way ANOVA, Tukey's multiple comparisons test. **e** Quantification of the latency to the first entrance to the previous shock zone and **f** the number shocks the animals would have received during the probe trial (day 6). The number of animals per genotype is the same in each graph and is indicated on the bar graphs. *$p < 0.05$, **$p < 0.01$, ***$p < 0.001$; two-way ANOVA, Tukey's multiple comparisons test

human-specific Aβ antibody 6E10. At 5.5 months of age, there were very few Aβ- and thioflavin-positive plaques in the cortex of APP/PS1 and p75^{KO}APP/PS1 mice (Fig. 3a–g). By 7.5 months of age, the plaque density and area had increased relative to the values obtained in the younger mice, but there was no significant difference between genotypes (Fig. 3a–g). These results indicate that loss of p75^{NTR} expression in cBF neurons does not result in earlier Aβ accumulation. However, at 11.5 months of age, the cortex of p75^{KO}APP/PS1 mice displayed both significantly reduced plaque density and a smaller plaque area than those of control APP/PS1 mice (Fig. 3a–g). This was accompanied by decreased astrocyte (Fig. 3h, i)(Fig. 3j, k), indicative of reduced gliosis.

To determine whether the reduction in plaque load was due to reduced production of Aβ, hippocampal lysates of 15-month-old mice were analyzed by ELISA for Aβ42, with no significant difference being found between APP/PS1 and p75^{KO}APP/PS1 mice (Fig. 4a). We also examined the levels of APP, ADAM10, and BACE1 in cortical (Fig. 4b) and hippocampal (data not shown) lysates of 12-month-old p75^{KO} and p75$^{fl/fl}$ mice. Western blotting did not reveal any significant change in the levels of these proteins (Fig. 4c). However, the ChAT protein levels in the cortical lysates were increased in p75^{KO} mice compared to cre-negative controls (Fig. 4b, c), demonstrating that our methods were sufficiently sensitive to detect a subtle change, consistent with the increase in cholinergic innovation to the cortex (Fig. 1d). Together, these

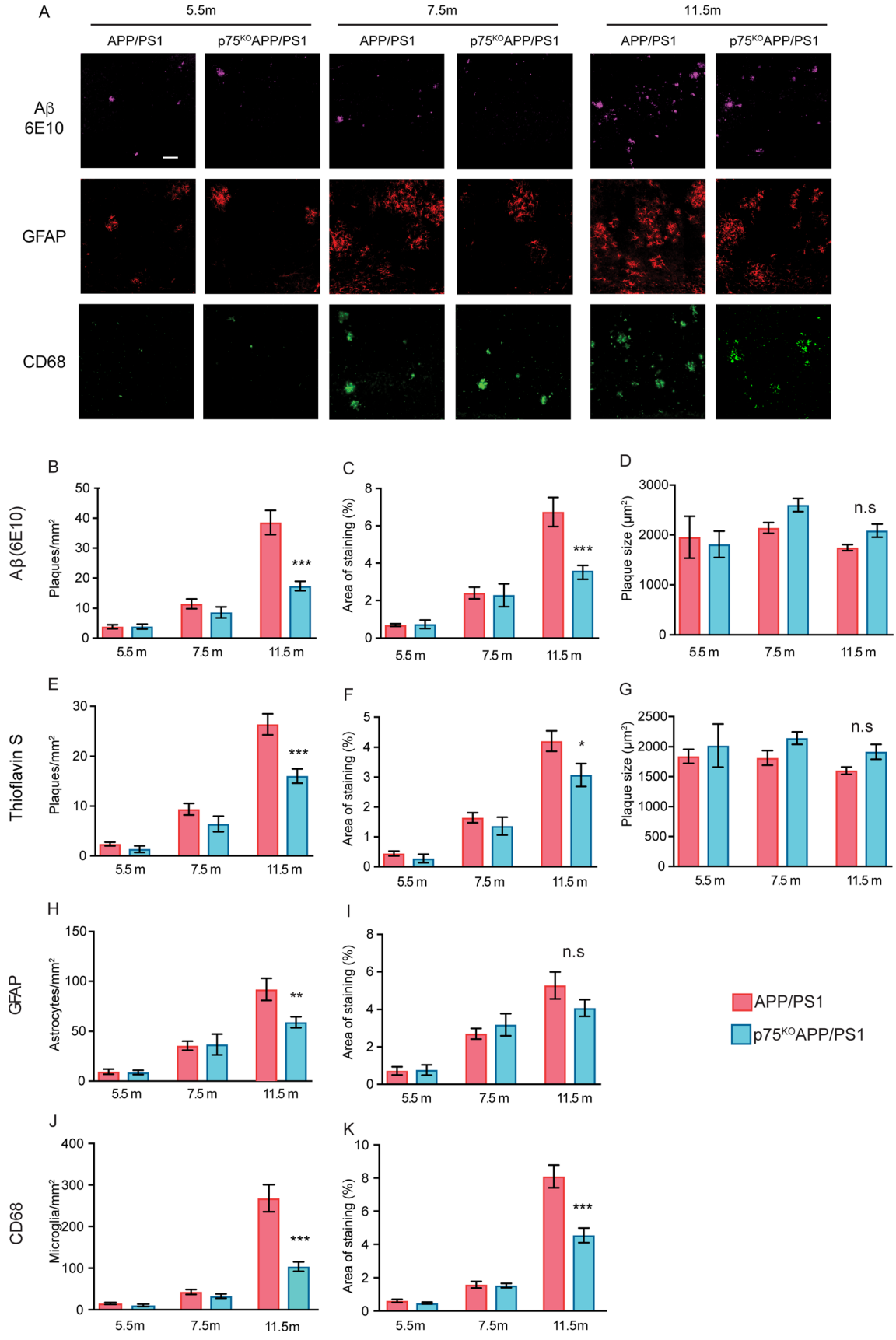
A
5.5m
7.5m
11.5m
APP/PS1
p75KOAPP/PS1
Aβ 6E10
GFAP
CD68
B
Aβ(6E10)
Plaques/mm²
C
Area of staining (%)
D
Plaque size (μm²)
n.s
E
Thioflavin S
F
G
H
GFAP
Astrocytes/mm²
I
J
CD68
Microglia/mm²
K
5.5 m
7.5 m
11.5 m
APP/PS1
p75KOAPP/PS1

◀ **Fig. 3** 6E10, GFAP, and CD68 immunostaining of coronal sections of the cortex of $p75^{fl/fl}$, APP/PS1, $p75^{KO}$, and $p75^{KO}$APP/PS1 animals at the indicated ages (**a**). Scale bars 100 μm. Quantification of amyloid plaque number (**b**, **e**), total area stained (**c**, **f**), and plaque size (**d**, **g**) following identification with Aβ antibody 6E10 (**b**–**d**) or thioflavin S (**e**–**g**) in motor and somatosensory cortical sections. Quantification of the number of (H) and area covered by (**i**) GFAP-positive astrocytes in cortical sections. Quantification of the number of (**j**) and area covered by (**k**) CD68-positive microglia $*p < 0.05$; $**p < 0.01$, $***p < 0.001$, two-way ANOVA, Tukey's multiple comparisons test. APP/PS1 vs $p75^{KO}$APP/PS1 5.5 m, $n = 3$ vs 6; 7.5 m, 8 vs 4; 11 m, 6 vs 6

findings suggest that Aβ deposition, rather than the rate of Aβ production, is decreased in the $p75^{KO}$APP/PS1 mice.

It has been shown that $p75^{ECD}$ can act to prevent Aβ aggregation and facilitate its clearance [35, 49]. As cBF neurons comprise the major cell type in the healthy adult brain to express $p75^{NTR}$, they are expected to be the main source of the $p75^{ECD}$ that is able to bind Aβ. Depletion of $p75^{NTR}$ from cBF neurons would therefore be expected to result in increased Aβ. To determine whether other sources of brain $p75^{ECD}$ can act to sequester Aβ (such as neurons or glia in the frontal cortex and hippocampus which upregulate $p75^{NTR}$ in AD [55–57]), $p75^{NTR}$ expression in 12-month-old C57BL6 and APP/PS1 mice was determined by immunohistochemistry. This revealed an increase in $p75^{NTR}$ levels within the cBF axons of APP/PS1 mice, as previously reported [58], with no other major cellular source of $p75^{NTR}$ being identified (Fig. 5a–d). As peripheral $p75^{ECD}$ can also sequester Aβ [21, 49], we next asked whether an increase in peripheral $p75^{ECD}$ production might explain our results. To investigate this, we measured the urinary levels of this fragment by ELISA. First, the amount of $p75^{ECD}$ in the urine of C57BL6 mice that had undergone cBF lesions (following injection of anti-$p75^{NTR}$-saporin toxin) was determined. No significant difference in the level of $p75^{ECD}$ was found between these lesioned mice and control animals (Fig. 5e), indicating that cBF neuron-derived $p75^{ECD}$ does not contribute significantly to the $p75^{ECD}$ found in urine. Next, to determine whether there was an upregulation of peripheral $p75^{ECD}$ in APP/PS1 mice that might contribute to sequestering Aβ, the amount of $p75^{ECD}$ in the urine of 13-month-old APP/PS1, $p75^{KO}$APP/PS1, and control mouse strains was determined. Although there was a trend for reduced $p75^{ECD}$ in $p75^{KO}$ mice (in which all cholinergic cells lack $p75^{NTR}$) compared to cre-negative $p75^{fl/fl}$ animals, there was no significant difference in the urinary level of $p75^{ECD}$ between the genotypes (Fig. 5e). These results indicate that the reduction in Aβ deposition in the brain is not due to an increase in brain or peripheral $p75^{ECD}$.

Discussion

Here, we report that conditional deletion of $p75^{NTR}$ from cholinergic neurons in APP/PS1 mice significantly delays cognitive impairment and reduces the deposition of transgenic

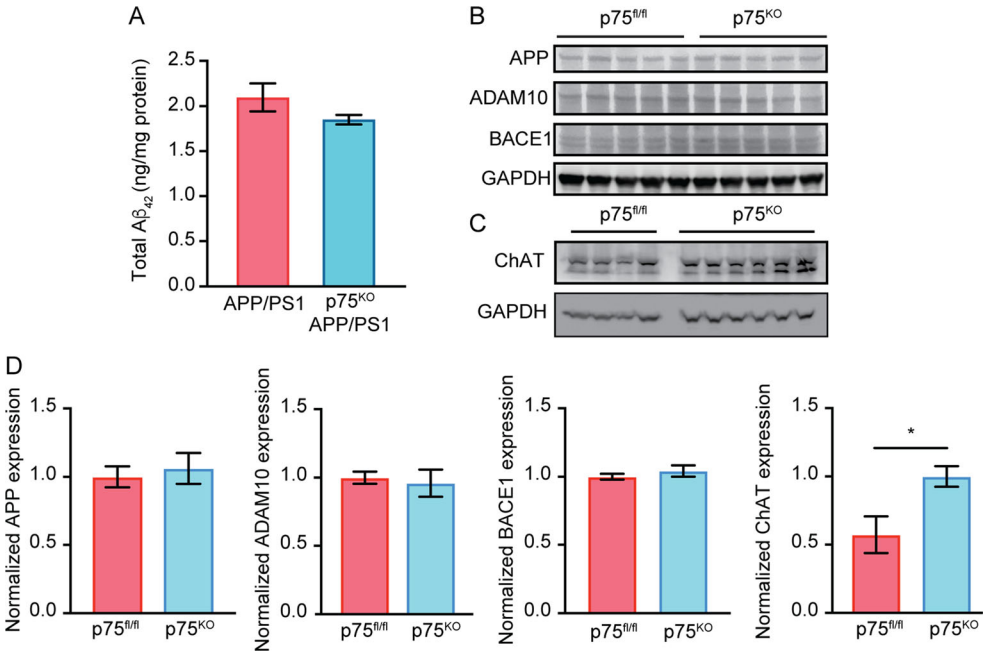

Fig. 4 **a** The total amount of Aβ42 in detergent-extracted cortical lysates, derived from 15-month-old mice, as quantified by ELISA. $n = 3$ per group. **b** Western blots of cortical lysates from 12- to 12.5-month-old $p75^{fl/fl}$ (WT) and ChAT-cre: $p75^{in/in}$ (KO) mice probed with antibodies for APP and α- and β-cleavage enzymes (ADAM10 and BACE1 respectively), ChAT, and the loading control GAPDH. Western blots of cortical lysates from 12.5-month-old mice probed with anti-ChAT antibody. **c**. Quantification of APP ADAM10, BACE1, and ChAT levels relative to GAPDH loading controls. A difference in intensity between genotypes was only observed for the ChAT protein.$*p < 0.05$, *t* test

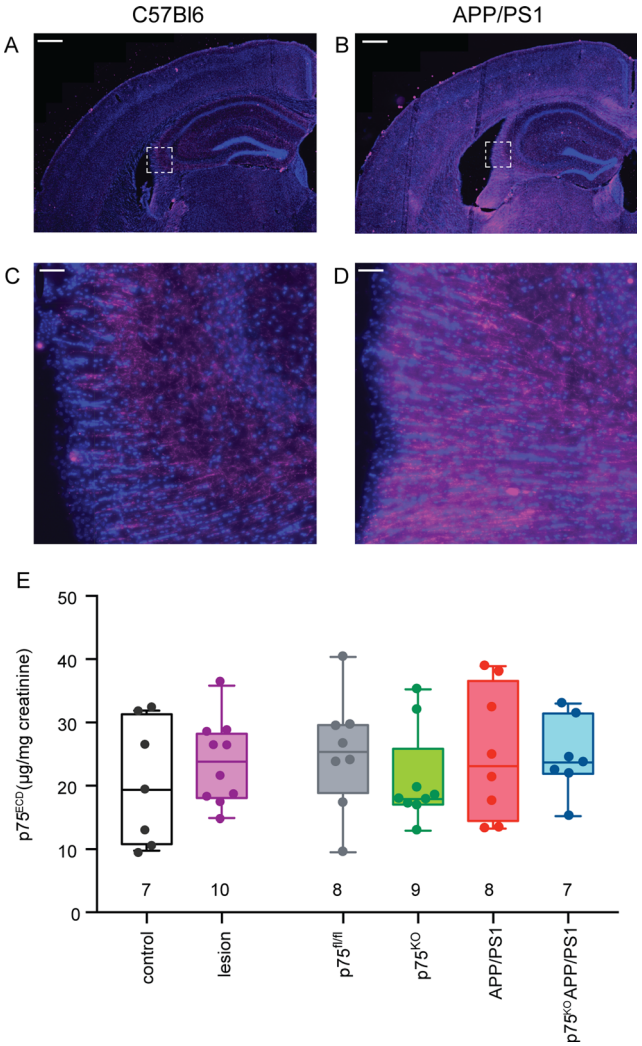

Fig. 5 Brain sections of 12-month-old **a**, **b** C57Bl6 and **c**, **d** APP/PS1 mice immunostained with an extracellular $p75^{NTR}$ antibody (pink) and a nuclear stain (DAPI; blue). **c**, **d** White boxes represent higher power images. Although $p75^{NTR}$-expressing cBF axons can clearly be seen, there are no other cell types expressing $p75^{NTR}$ in the brain. Scale bars: **a** and **b**, 500 µm; **c** and **d**, 50 µm. **e** Quantification of the amount of $p75^{ECD}$ in the urine of 5-month-old C57BL6 mice injected with either IgG-saporin (control) or p75-saporin (lesion) 4 weeks earlier, and 13-month-old mice of various genotypes. No significant differences were found between control and lesion (two-way *t* test) or genotype (one-way ANOVA, Sidak's multiple comparisons test). The number of mice in each group is indicated

APP-derived Aβ into plaques in the cortex. Analysis of total Aβ levels, together with the expression of APP and BACE1 suggest that these phenotypes are not due to either decreased Aβ production or Aβ sequestration by $p75^{ECD}$ fragments. Rather, we suggest that the depletion of $p75^{NTR}$ from cholinergic neurons alters cBF neuron function, which slows the processes that cause cognitive impairment and increase Aβ clearance from the brains of $p75^{KO}$ APP/PS1 mice.

Our first finding was that the significant cognitive deficits observed in aged APP/PS1 mice subjected to the active place avoidance task were reduced by postnatal loss of $p75^{NTR}$ from cholinergic neurons. Although the animal numbers per group are limited, the trend for improved behavior in the active place avoidance task is consistent with those of a number of studies which have reported that systemic removal or downregulation of $p75^{NTR}$ expression results in positive spatial memory outcomes compared with age-matched cognitively impaired Aβ-overproducing littermates (Table 1). However as cBF neurons are the principal neurons of the brain to express $p75^{NTR}$, it not surprising that the behavioral changes observed in complete $p75^{KO}$ mice have been replicated using our cholinergic-specific conditional $p75^{KO}$ mouse. Furthermore, it is likely that the reduction in $p75^{NTR}$ signaling in cBF neurons is responsible for the previous results observed when $p75^{NTR}$ is downregulated globally. Indeed, a number of studies have demonstrated that genetic removal or downregulation of $p75^{NTR}$ can enhance outcomes in learning and memory tasks in otherwise wild-type mice [41, 59], including our ChAT-cre; $p75^{in/in}$ mice [39, 60]. Such findings are also consistent with the loss of $p75^{NTR}$ function enhancing long-term potentiation and/or reducing long-term depression, including in the context of increased Aβ [31, 37, 61, 62]. However, differences between genotypes were not observed in the Y-maze task, which is also hippocampal-dependent but less reliant on cBF neurons [40]. This indicates that the loss of $p75^{NTR}$ in the brain, and specifically within cBF neurons, has a significant effect on cognitive processing that enhances memory, which is dominant over any negative effects of Aβ or related AD pathology.

Although most previous studies have reported cognitive improvements in AD transgenic mice when $p75^{NTR}$ function is inhibited, there is no consensus on the effect on Aβ levels (Table 1). This may be partially due to the use of different strains of Aβ overproducing mice and their genetic backgrounds, as well as the methods used by independent groups to monitor Aβ. Nonetheless, based on the ability of $p75^{NTR}$ to bind and sequester Aβ, we hypothesized that the loss of cBF $p75^{NTR}$ would result in exacerbated Aβ accumulation. However, an equivalent total Aβ level was found in the hippocampus of 15-month-old APP/PS1 and $p75^{KO}$APP/PS1 mice when measured by ELISA. Given the reduction in Aβ plaque levels between 7 and 11.5 months, this could indicate an increase in soluble Aβ levels.

Soluble Aβ is known to be the more neurotoxic species and has been associated with impaired long-term potentiation and cognitive processes [63]. However, as the $p75^{KO}$APP/PS1 animals displayed partial cognitive improvements, rather than exacerbation of the impairment, it is unlikely that any increase in soluble Aβ is significant. Although it is not possible to conclusively determine whether the behavioral improvement is due to the reduced Aβ plaque load and/or to changes in cBF function, cognitive improvements have been reported in AD mouse models with reduced $p75^{NTR}$ function, even when there is no change or an increase in Aβ plaque load [20, 37], suggesting that these two phenotypes are independent.

Therefore, our study indicates that preventing $p75^{NTR}$ expression in cBF neurons specifically provides two positive outcomes in the context of AD: a reduction in Aβ plaques and improved spatial memory.

How might cBF $p75^{NTR}$ reduce Aβ plaque load? Similar to our findings, Jian and colleagues reported reduced Aβ plaque load and improved spatial memory in $p75^{NTR+/-}$ Tg2576 mice [38], with no change in ADAM10 or BACE1 expression. However, they observed reduced levels of both soluble and plaque Aβ, which was accounted for by reduced activity of β-secretase and PS1. Wang and colleagues [35] also reported no change in BACE1 levels in complete $p75^{NTR-/-}$ APP/PS1 mice, but a significant increase in total Aβ levels. In our study, it is possible that the combination of genetic changes altered the expression or activity of cleavage enzymes, including cortical area- or layer-specific changes in the $p75^{KO}$APP/PS1 mice that were not detected by our methods. However, the lack of change in total Aβ levels in $p75^{KO}$APP/PS1 mice compared to APP/PS1 animals indicates that altered cleavage of APP does not appreciably account for the reduced plaque load observed in the former mice. Rather, the results imply that Aβ clearance mechanisms are enhanced in our transgenic mice.

Reduced clearance of Aβ is considered a major mediator of idiopathic AD [64]. $p75^{NTR}$-mediated endocytosis and degradation of Aβ within cBF neurons has been proposed as a major mechanism regulating the physiological levels of Aβ within brain areas innervated by cBF axons [22]. An additional role for cleaved $p75^{ECD}$ in reducing Aβ deposition has also been demonstrated [49]. In our paradigm, $p75^{NTR}$-mediated sequestration of Aβ by cBF neurons was not possible. Furthermore, the level of $p75^{ECD}$, as indicated by the level of this fragment in the urine, was not significantly reduced by cholinergic-specific $p75^{NTR}$ knockdown or cBF lesioning, and peripheral levels of $p75^{NTR}$ were not appreciably upregulated in the $p75^{KO}$APP/PS1 mice. Similarly, it has been reported that treatment with the $p75^{NTR}$-inhibiting compound LM11A-31, which induces cleavage of $p75^{NTR}$ [19], does not significantly alter total hippocampal Aβ levels in AD model mice [19]. This signifies that interactions between cBF-derived $p75^{NTR}$ and Aβ do not appreciably regulate Aβ load. We do not refute the possibility that cBF neuronal $p75^{NTR}$ internalizes Aβ, or that $p75^{ECD}$ can reduce Aβ aggregation. However, our data indicate that another, more dominant Aβ clearance mechanism is mediated by the loss of $p75^{NTR}$ from cBF neurons.

Another Aβ clearance mechanism is phagocytic removal by microglia [65, 66]. In our paradigm, the number of activated microglia (and astrocytes) was significantly reduced in $p75^{KO}$APP/PS1 mice compared to their APP/PS1 littermates, suggesting that this process is not active. This result also suggests that Aβ does not aggregate as plaques before being removed by inflammation-driven mechanisms, but rather that soluble Aβ is cleared prior to aggregation and deposition. LM11A-31 treatment has also been shown to decrease the activation of microglia and to attenuate the levels of reactive astrocytes [36] without changing total Aβ levels [19]. It is therefore possible that microglia in $p75^{NTR}$-deficient tissue can actively remove Aβ without transformation into the deleterious microglial phenotype associated with aging and AD [66]. The possibility of a decreased hyper-inflammatory response mediated by loss of $p75^{NTR}$ signaling [57] also warrants further investigation.

$p75^{NTR}$ is known to affect cBF neuron number and structure, with both complete and conditional $p75^{KO}$ mice having ~25% more cBF neurons and significantly increased innervation of the cortex [39, 60]. This is the likely explanation for the improvement in spatial memory exhibited by our $p75^{KO}$APP/PS1 mice. Enhanced cholinergic signaling has also been shown to affect Aβ levels, although predominantly by altering APP cleavage. For example, muscarinic M1 receptor agonists reverse Aβ pathology in 3 × Tg AD model mice, by enhancing α-secretase cleavage of APP [67]. Genetic deletion of M1 receptors in the $APP^{Swedish/Indiana}$ AD mouse model also induces exacerbated Aβ-related pathology [68]. In addition, knockout of the cholinergic vesicle transporter changes cBF neuron-derived microRNAs, including affecting BACE1 expression [69, 70]. As indicated above, it is possible that such changes in APP cleavage occurred in our mice but were not detected experimentally. However, an alternative explanation is that cholinergic neurons regulate mechanisms of Aβ clearance, which are currently incompletely understood. Both Aβ-degrading enzymes, such as neprilysin, and glymphatic drainage of neural waste such as Aβ from interstitial fluid are attracting increasing interest as processes that affect Aβ accumulation [71, 72]. cBF neurons directly innervate the neocortical microvessels, releasing acetylcholine which is an important regulator of cerebral blood flow and vessel dilation [72, 73]. In turn, cholinergic regulation of blood flow might affect glymphatic drainage and/or the availability of circulating neprilysin to clear brain Aβ [74]. This is a speculative, but attractive, explanation of our findings.

In summary, we have found that removal of $p75^{NTR}$ expression from cholinergic neurons during the postnatal and adult life of the familial AD model mice reduces cortical Aβ deposition and gliosis without changing the production of Aβ, and slows cognitive impairment in aged animals. We propose that the Aβ clearance mechanisms in our $p75^{KO}$ APP/PS1 mice are enhanced due to increased cholinergic innovation and function. Targeting $p75^{NTR}$ to promote cholinergic function may therefore have a dual effect of inhibiting cBF neuronal degeneration and promoting Aβ clearance.

Acknowledgements We thank other members of our laboratories, particularly Bree Rumballe (Coulson Lab) and Micell Cardoso (Rogers Lab) for administrative and technical assistance respectively, as well as helpful discussions, Luke Hammond for assistance with microscopy analysis and Rowan Tweedale for critical reading and editing of the manuscript.

Funding This work was supported by the Australian National Health and Medical Research Council of Australia [project grant 1049236 to EJC; project grant 1139469 and Boosting Dementia Fellowship 1139469 to RM], and a Motor Neuron Disease Australia Grant in Aid [MLR,SS].

Compliance with Ethical Standards

All procedures were approved by the University of Queensland Animal Ethics Committee and conducted in accordance with the Australian Code of Practice for the Care and Use of Animals for Scientific Purposes.

Conflict of Interest The authors declare no competing interests.

References

1. Whitehouse PJ, Struble RG, Clark AW, Price DL (1982) Alzheimer disease: plaques, tangles, and the basal forebrain. Ann Neurol 12(5):494. https://doi.org/10.1002/ana.410120517
2. Grothe MJ, Schuster C, Bauer F, Heinsen H, Prudlo J, Teipel SJ (2014) Atrophy of the cholinergic basal forebrain in dementia with Lewy bodies and Alzheimer's disease dementia. J Neurol 261(10): 1939–1948. https://doi.org/10.1007/s00415-014-7439-z
3. Grothe M, Heinsen H, Teipel S (2013) Longitudinal measures of cholinergic forebrain atrophy in the transition from healthy aging to Alzheimer's disease. Neurobiol Aging 34(4):1210–1220. https://doi.org/10.1016/j.neurobiolaging.2012.10.018
4. Mufson EJ, Ma SY, Dills J, Cochran EJ, Leurgans S, Wuu J, Bennett DA, Jaffar S et al (2002) Loss of basal forebrain $p75^{NTR}$ immunoreactivity in subjects with mild cognitive impairment and Alzheimer's disease. J Comp Neurol 443(2):136–153
5. Schmitz TW, Nathan Spreng R, Alzheimer's Disease Neuroimaging I (2016) Basal forebrain degeneration precedes and predicts the cortical spread of Alzheimer's pathology. Nat Commun 7:13249. https://doi.org/10.1038/ncomms13249
6. Grothe M, Zaborszky L, Atienza M, Gil-Neciga E, Rodriguez-Romero R, Teipel SJ, Amunts K, Suarez-Gonzalez A et al (2010) Reduction of basal forebrain cholinergic system parallels cognitive impairment in patients at high risk of developing Alzheimer's disease. Cereb Cortex 20(7):1685–1695. https://doi.org/10.1093/cercor/bhp232
7. Grothe MJ, Ewers M, Krause B, Heinsen H, Teipel SJ, Alzheimer's Disease Neuroimaging I (2014) Basal forebrain atrophy and cortical amyloid deposition in nondemented elderly subjects. Alzheimers Dement 10(5 Suppl):S344–S353. https://doi.org/10.1016/j.jalz.2013.09.011
8. Teipel S, Heinsen H, Amaro E Jr, Grinberg LT, Krause B, Grothe M, Alzheimer's Disease Neuroimaging I (2014) Cholinergic basal forebrain atrophy predicts amyloid burden in Alzheimer's disease. Neurobiol Aging 35(3):482–491. https://doi.org/10.1016/j.neurobiolaging.2013.09.029
9. Teipel SJ, Meindl T, Grinberg L, Grothe M, Cantero JL, Reiser MF, Moller HJ, Heinsen H et al (2011) The cholinergic system in mild cognitive impairment and Alzheimer's disease: An in vivo MRI and DTI study. Hum Brain Mapp 32(9):1349–1362. https://doi.org/10.1002/hbm.21111
10. Kerbler GM, Fripp J, Rowe CC, Villemagne VL, Salvado O, Rose S, Coulson EJ, Alzheimer's Disease Neuroimaging I (2015) Basal forebrain atrophy correlates with amyloid β burden in Alzheimer's disease. NeuroImage Clin 7:105–113. https://doi.org/10.1016/j.nicl.2014.11.015
11. Kerbler GM, Nedelska Z, Fripp J, Laczo J, Vyhnalek M, Lisy J, Hamlin AS, Rose S et al (2015) Basal forebrain atrophy contributes to allocentric navigation impairment in Alzheimer's disease patients. Front Aging Neurosci 7:185. https://doi.org/10.3389/fnagi.2015.00185
12. Laursen B, Mork A, Plath N, Kristiansen U, Bastlund JF (2013) Cholinergic degeneration is associated with increased plaque deposition and cognitive impairment in APPswe/PS1dE9 mice. Behav Brain Res 240:146–152. https://doi.org/10.1016/j.bbr.2012.11.012
13. Gil-Bea FJ, Gerenu G, Aisa B, Kirazov LP, Schliebs R, Ramirez MJ (2012) Cholinergic denervation exacerbates amyloid pathology and induces hippocampal atrophy in Tg2576 mice. Neurobiol Dis 48(3):439–446. https://doi.org/10.1016/j.nbd.2012.06.020
14. Hartig W, Saul A, Kacza J, Grosche J, Goldhammer S, Michalski D, Wirths O (2014) Immunolesion-induced loss of cholinergic projection neurones promotes β-amyloidosis and tau hyperphosphorylation in the hippocampus of triple-transgenic mice. Neuropathol Appl Neurobiol 40(2):106–120. https://doi.org/10.1111/nan.12050
15. Ramos-Rodriguez JJ, Pacheco-Herrero M, Thyssen D, Murillo-Carretero MI, Berrocoso E, Spires-Jones TL, Bacskai BJ, Garcia-Alloza M (2013) Rapid β-amyloid deposition and cognitive impairment after cholinergic denervation in APP/PS1 mice. J Neuropathol Exp Neurol 72(4):272–285. https://doi.org/10.1097/NEN.0b013e318288a8dd
16. Turnbull MT, Boskovic Z, Coulson EJ (2018) Acute down-regulation of BDNF signaling does not replicate exacerbated amyloid-β levels and cognitive impairment induced by cholinergic basal forebrain lesion. Front Mol Neurosci 11:51. https://doi.org/10.3389/fnmol.2018.00051
17. Hernandez CM, Kayed R, Zheng H, Sweatt JD, Dineley KT (2010) Loss of α7 nicotinic receptors enhances β-amyloid oligomer accumulation, exacerbating early-stage cognitive decline and septohippocampal pathology in a mouse model of Alzheimer's disease. J Neurosci 30(7):2442–2453. https://doi.org/10.1523/JNEUROSCI.5038-09.2010
18. Sotthibundhu A, Sykes AM, Fox B, Underwood CK, Thangnipon W, Coulson EJ (2008) β-$amyloid_{1-42}$ induces neuronal death through the p75 neurotrophin receptor. J Neurosci 28(15):3941–3946
19. Knowles JK, Simmons DA, Nguyen TV, Vander Griend L, Xie Y, Zhang H, Yang T, Pollak J et al (2013) A small molecule p75 ligand prevents cognitive deficits and neurite degeneration in an Alzheimer's mouse model. Neurobiol Aging 34:2052–2063. https://doi.org/10.1016/j.neurobiolaging.2013.02.015
20. Knowles JK, Rajadas J, Nguyen TV, Yang T, LeMieux MC, Vander Griend L, Ishikawa C, Massa SM et al (2009) The p75 neurotrophin receptor promotes amyloid-β_{1-42}-induced neuritic dystrophy in vitro and in vivo. J Neurosci 29(34):10627–10637. https://doi.org/10.1523/JNEUROSCI.0620-09.2009
21. Ovsepian SV, Antyborzec I, O'Leary VB, Zaborszky L, Herms J, Oliver Dolly J (2014) Neurotrophin receptor p75 mediates the uptake of the amyloid beta (Aβ) peptide, guiding it to lysosomes for degradation in basal forebrain cholinergic neurons. Brain Struct Funct 219(5):1527–1541. https://doi.org/10.1007/s00429-013-0583-x
22. Ovsepian SV, Herms J (2013) Drain of the brain: low-affinity p75 neurotrophin receptor affords a molecular sink for clearance of cortical amyloid β by the cholinergic modulator system. Neurobiol Aging 34(11):2517–2524. https://doi.org/10.1016/j.neurobiolaging.2013.05.005

23. Ibanez CF, Simi A (2012) p75 neurotrophin receptor signaling in nervous system injury and degeneration: paradox and opportunity. Trends Neurosci 35(7):431–440. https://doi.org/10.1016/j.tins.2012.03.007
24. Dechant G, Barde YA (2002) The neurotrophin receptor p75^{NTR}: novel functions and implications for diseases of the nervous system. Nat Neurosci 5(11):1131–1136
25. Coulson EJ, May LM, Sykes AM, Hamlin AS (2009) The role of the p75 neurotrophin receptor in cholinergic dysfunction in Alzheimer's disease. Neuroscientist 15(4):317–323. https://doi.org/10.1177/1073858408331376
26. Yaar M, Zhai S, Pilch PF, Doyle SM, Eisenhauer PB, Fine RE, Gilchrest BA (1997) Binding of β-amyloid to the p75 neurotrophin receptor induces apoptosis. A possible mechanism for Alzheimer's disease. J Clin Invest 100(9):2333–2340
27. Yaar M, Zhai S, Fine RE, Eisenhauer PB, Arble BL, Stewart KB, Gilchrest BA (2002) Amyloid β binds trimers as well as monomers of the 75-kDa neurotrophin receptor and activates receptor signaling. J Biol Chem 277(10):7720–7725
28. Wang YR, Wang J, Liu YH, Hu GL, Gao CY, Wang YJ, Zhou XF, Zeng F (2018) Cysteine-rich repeat domains 2 and 4 are amyloid-β binding domains of neurotrophin receptor p75^{NTR} and potential targets to block amyloid-β neurotoxicity. J Alzheimers Dis 63(1):139–147. https://doi.org/10.3233/JAD-171012
29. Rabizadeh S, Bitler CM, Butcher LL, Bredesen DE (1994) Expression of the low-affinity nerve growth factor receptor enhances β-amyloid peptide toxicity. Proc Natl Acad Sci U S A 91(22):10703–10706
30. May LM, Anggono V, Gooch HM, Jang SE, Matusica D, Kerbler GM, Meunier FA, Sah P et al (2017) G-protein-coupled inwardly rectifying potassium (GIRK) channel activation by the p75 neurotrophin receptor is required for amyloid β toxicity. Front Neurosci 11:455. https://doi.org/10.3389/fnins.2017.00455
31. Yang T, Knowles JK, Lu Q, Zhang H, Arancio O, Moore LA, Chang T, Wang Q et al (2008) Small molecule, non-peptide p75 ligands inhibit Aβ-induced neurodegeneration and synaptic impairment. PLoS One 3(11):e3604. https://doi.org/10.1371/journal.pone.0003604
32. Costantini C, Rossi F, Formaggio E, Bernardoni R, Cecconi D, Della-Bianca V (2005) Characterization of the signaling pathway downstream p75 neurotrophin receptor involved in β-amyloid peptide-dependent cell death. J Mol Neurosci 25(2):141–156
33. Kuner P, Schubenel R, Hertel C (1998) β-amyloid binds to p75^{NTR} and activates NFκB in human neuroblastoma cells. J Neurosci Res 54(6):798–804
34. Hu Y, Lee X, Shao Z, Apicco D, Huang G, Gong BJ, Pepinsky RB, Mi S (2013) A DR6/p75^{NTR} complex is responsible for β-amyloid-induced cortical neuron death. Cell Death Dis 4:e579. https://doi.org/10.1038/cddis.2013.110
35. Wang YJ, Wang X, Lu JJ, Li QX, Gao CY, Liu XH, Sun Y, Yang M et al (2011) p75NTR regulates Aβ deposition by increasing Aβ production but inhibiting Aβ aggregation with its extracellular domain. J Neurosci 31(6):2292–2304. https://doi.org/10.1523/JNEUROSCI.2733-10.2011
36. Nguyen TV, Shen L, Vander Griend L, Quach LN, Belichenko NP, Saw N, Yang T, Shamloo M et al (2014) Small molecule p75^{NTR} ligands reduce pathological phosphorylation and misfolding of tau, inflammatory changes, cholinergic degeneration, and cognitive deficits in AβPP(L/S) transgenic mice. J Alzheimers Dis 42(2):459–483. https://doi.org/10.3233/JAD-140036
37. Murphy M, Wilson YM, Vargas E, Munro KM, Smith B, Huang A, Li QX, Xiao J et al (2015) Reduction of p75 neurotrophin receptor ameliorates the cognitive deficits in a model of Alzheimer's disease. Neurobiol Aging 36(2):740–752. https://doi.org/10.1016/j.neurobiolaging.2014.09.014
38. Jian C, Zou D, Luo C, Liu X, Meng L, Huang J, Li X, Huang R et al (2016) Cognitive deficits are ameliorated by reduction in amyloid β accumulation in Tg2576/p75$^{NTR+/-}$ mice. Life Sci 155:167–173. https://doi.org/10.1016/j.lfs.2016.05.011
39. Boskovic Z, Alfonsi F, Rumballe BA, Fonseka S, Windels F, Coulson EJ (2014) The role of p75^{NTR} in cholinergic basal forebrain structure and function. J Neurosci 34(39):13033–13038. https://doi.org/10.1523/JNEUROSCI.2364-14.2014
40. Hamlin AS, Windels F, Boskovic Z, Sah P, Coulson EJ (2013) Lesions of the basal forebrain cholinergic system in mice disrupt idiothetic navigation. PLoS One 8(1):e53472. https://doi.org/10.1371/journal.pone.0053472
41. Greferath U, Bennie A, Kourakis A, Bartlett PF, Murphy M, Barrett GL (2000) Enlarged cholinergic forebrain neurons and improved spatial learning in p75 knockout mice. Eur J Neurosci 12(3):885–893
42. Longo FM, Massa SM (2013) Small-molecule modulation of neurotrophin receptors: a strategy for the treatment of neurological disease. Nat Rev Drug Discov 12(7):507–525
43. Zeng F, Lu JJ, Zhou XF, Wang YJ (2011) Roles of p75^{NTR} in the pathogenesis of Alzheimer's disease: a novel therapeutic target. Biochem Pharmacol 82(10):1500–1509. https://doi.org/10.1016/j.bcp.2011.06.040
44. Mufson EJ, Counts SE, Perez SE, Ginsberg SD (2008) Cholinergic system during the progression of Alzheimer's disease: therapeutic implications. Expert Rev Neurother 8(11):1703–1718. https://doi.org/10.1586/14737175.8.11.1703
45. Shepheard SR, Wuu J, Cardoso M, Wiklendt L, Dinning PG, Chataway T, Schultz D, Benatar M et al (2017) Urinary p75^{ECD}: a prognostic, disease progression, and pharmacodynamic biomarker in ALS. Neurology 88(12):1137–1143. https://doi.org/10.1212/WNL.0000000000003741
46. Jiao SS, Bu XL, Liu YH, Wang QH, Liu CH, Yao XQ, Zhou XF, Wang YJ (2015) Differential levels of p75^{NTR} ectodomain in CSF and blood in patients with Alzheimer's disease: a novel diagnostic marker. Transl Psychiatry 5:e650. https://doi.org/10.1038/tp.2015.146
47. Zhou XF, Wang YJ (2011) The p75^{NTR} extracellular domain: a potential molecule regulating the solubility and removal of amyloid-β. Prion 5(3):161–163
48. Wang QH, Wang YR, Zhang T, Jiao SS, Liu YH, Zeng F, Li J, Yao XQ et al (2016) Intramuscular delivery of p75^{NTR} ectodomain by an AAV vector attenuates cognitive deficits and Alzheimer's disease-like pathologies in APP/PS1 transgenic mice. J Neurochem 138(1):163–173. https://doi.org/10.1111/jnc.13616
49. Yao XQ, Jiao SS, Saadipour K, Zeng F, Wang QH, Zhu C, Shen LL, Zeng GH et al (2015) p75^{NTR} ectodomain is a physiological neuroprotective molecule against amyloid-β toxicity in the brain of Alzheimer's disease. Mol Psychiatry 20(11):1301–1310. https://doi.org/10.1038/mp.2015.49
50. Cimadevilla JM, Kaminsky Y, Fenton A, Bures J (2000) Passive and active place avoidance as a tool of spatial memory research in rats. J Neurosci Meth 102(2):155–164
51. Wesierska M, Dockery C, Fenton AA (2005) Beyond memory, navigation, and inhibition: behavioral evidence for hippocampus-dependent cognitive coordination in the rat. J Neurosci 25(9):2413–2419. https://doi.org/10.1523/JNEUROSCI.3962-04.2005
52. Shepheard SR, Chataway T, Schultz DW, Rush RA, Rogers ML (2014) The extracellular domain of neurotrophin receptor p75 as a candidate biomarker for amyotrophic lateral sclerosis. PLoS One 9(1):e87398. https://doi.org/10.1371/journal.pone.0087398
53. Matusica D, Alfonsi F, Turner BJ, Butler TJ, Shepheard SR, Rogers ML, Skeldal S, Underwood CK et al (2016) Inhibition of motor neuron death in vitro and in vivo by a p75 neurotrophin receptor intracellular domain fragment. J Cell Sci 129(3):517–530. https://doi.org/10.1242/jcs.173864

54. Vukovic J, Borlikova GG, Ruitenberg MJ, Robinson GJ, Sullivan RK, Walker TL, Bartlett PF (2013) Immature doublecortin-positive hippocampal neurons are important for learning but not for remembering. J Neurosci 33(15):6603–6613. https://doi.org/10.1523/JNEUROSCI.3064-12.2013
55. Mufson EJ, Kordower JH (1992) Cortical neurons express nerve growth factor receptors in advanced age and Alzheimer disease. Proc Natl Acad Sci U S A 89(2):569–573
56. Chakravarthy B, Gaudet C, Menard M, Atkinson T, Brown L, Laferla FM, Armato U, Whitfield J (2010) Amyloid-β peptides stimulate the expression of the $p75^{NTR}$ neurotrophin receptor in SHSY5Y human neuroblastoma cells and AD transgenic mice. J Alz Dis 19(3):915–925. https://doi.org/10.3233/JAD-2010-1288
57. Perini G, Della-Bianca V, Politi V, Della Valle G, Dal-Pra I, Rossi F, Armato U (2002) Role of p75 neurotrophin receptor in the neurotoxicity by β-amyloid peptides and synergistic effect of inflammatory cytokines. J Exp Med 195(7):907–918
58. Jaffar S, Counts SE, Ma SY, Dadko E, Gordon MN, Morgan D, Mufson EJ (2001) Neuropathology of mice carrying mutant APP^{swe} and/or $PS1^{M146L}$ transgenes: alterations in the $p75^{NTR}$ cholinergic basal forebrain septohippocampal pathway. Exp Neurol 170(2):227–243
59. Catts VS, Al-Menhali N, Burne TH, Colditz MJ, Coulson EJ (2008) The p75 neurotrophin receptor regulates hippocampal neurogenesis and related behaviours. Eur J Neurosci 28(5):883–892. https://doi.org/10.1111/j.1460-9568.2008.06390.x
60. Boskovic Z, Milne M, Qian L, Clifton H, McGovern AE, Turnbull MT, Mazzone SB, Coulson EJ (2018) Cholinergic basal forebrain neurons regulate fear extinction consolidation through p75 neurotrophin receptor signaling. Transl Psychiatry 8:199. https://doi.org/10.1038/s41398-018-0248-x, https://www.nature.com/articles/s41398-018-0248-x
61. Rosch H, Schweigreiter R, Bonhoeffer T, Barde YA, Korte M (2005) The neurotrophin receptor $p75^{NTR}$ modulates long-term depression and regulates the expression of AMPA receptor subunits in the hippocampus. Proc Natl Acad Sci U S A 102(20):7362–7367
62. Woo NH, Teng HK, Siao CJ, Chiaruttini C, Pang PT, Milner TA, Hempstead BL, Lu B (2005) Activation of p75NTR by proBDNF facilitates hippocampal long-term depression. Nat Neurosci 8(8):1069–1077
63. Mucke L, Masliah E, Yu GQ, Mallory M, Rockenstein EM, Tatsuno G, Hu K, Kholodenko D et al (2000) High-level neuronal expression of Aβ1-42 in wild-type human amyloid protein precursor transgenic mice: synaptotoxicity without plaque formation. J Neurosci 20(11):4050–4058
64. Agholme L, Hallbeck M (2014) Getting rid of intracellular Aβ - loss of cellular degradation leads to transfer between connected neurons. Curr Pharm Des 20(15):2458–2468
65. Zuroff L, Daley D, Black KL, Koronyo-Hamaoui M (2017) Clearance of cerebral Aβ in Alzheimer's disease: reassessing the role of microglia and monocytes. Cell Mol Life Sci 74(12):2167–2201. https://doi.org/10.1007/s00018-017-2463-7
66. Solito E, Sastre M (2012) Microglia function in Alzheimer's disease. Front Pharmacol 3:14. https://doi.org/10.3389/fphar.2012.00014
67. Caccamo A, Oddo S, Billings LM, Green KN, Martinez-Coria H, Fisher A, LaFerla FM (2006) M1 receptors play a central role in modulating AD-like pathology in transgenic mice. Neuron 49(5):671–682. https://doi.org/10.1016/j.neuron.2006.01.020
68. Davis AA, Fritz JJ, Wess J, Lah JJ, Levey AI (2010) Deletion of M1 muscarinic acetylcholine receptors increases amyloid pathology in vitro and in vivo. J Neurosci 30(12):4190–4196. https://doi.org/10.1523/JNEUROSCI.6393-09.2010
69. Kolisnyk B, Al-Onaizi MA, Xu J, Parfitt GM, Ostapchenko VG, Hanin G, Soreq H, Prado MA et al (2016) Cholinergic regulation of hnRNPA2/B1 translation by M1 muscarinic receptors. J Neurosci 36(23):6287–6296. https://doi.org/10.1523/JNEUROSCI.4614-15.2016
70. Kolisnyk B, Al-Onaizi M, Soreq L, Barbash S, Bekenstein U, Haberman N, Hanin G, Kish MT et al (2017) Cholinergic surveillance over hippocampal RNA metabolism and Alzheimer's-like pathology. Cereb Cortex 27(7):3553–3567. https://doi.org/10.1093/cercor/bhw177
71. Iliff JJ, Wang M, Liao Y, Plogg BA, Peng W, Gundersen GA, Benveniste H, Vates GE et al (2012) A paravascular pathway facilitates CSF flow through the brain parenchyma and the clearance of interstitial solutes, including amyloid β. Sci Transl Med 4(147):147ra111. https://doi.org/10.1126/scitranslmed.3003748
72. Peng W, Achariyar TM, Li B, Liao Y, Mestre H, Hitomi E, Regan S, Kasper T et al (2016) Suppression of glymphatic fluid transport in a mouse model of Alzheimer's disease. Neurobiol Dis 93:215–225. https://doi.org/10.1016/j.nbd.2016.05.015
73. Hamner JW, Tan CO, Tzeng YC, Taylor JA (2012) Cholinergic control of the cerebral vasculature in humans. J Physiol 590(24):6343–6352. https://doi.org/10.1113/jphysiol.2012.245100
74. Liu Y, Studzinski C, Beckett T, Murphy MP, Klein RL, Hersh LB (2010) Circulating neprilysin clears brain amyloid. Mol Cell Neurosci 45(2):101–107. https://doi.org/10.1016/j.mcn.2010.05.014